

## STABILITY ANALYSIS OF A ROTATING FLOW TOWARD A SHRINKING PERMEABLE SURFACE IN NANOFUID

Siti Nur Alwani Salleh\*, Norfifah Bachok, and Norihan Md Arifin

Department of Mathematics and Institute for Mathematical Research, Universiti Putra Malaysia, 43400 UPM Serdang, Selangor, Malaysia

\*Corresponding Author: alwani24salleh@gmail.com

Received: 28<sup>th</sup> Oct 2018

Revised: 28<sup>th</sup> Oct 2018

Accepted 19<sup>th</sup> Dec 2018

DOI: <https://doi.org/10.22452/mjs.sp2019no1.2>

**ABSTRACT** The rotating boundary layer flow over a shrinking permeable surface in nanofluid is numerically studied. The similarity transformation is used to transform the partial differential equations into nonlinear ordinary differential equations. Later, these equations are determined by using bvp4c package in the MATLAB software. The numerical results reveal that there is more than one solution called dual solutions obtained for a certain range of the rotation and suction parameters. A stability analysis is performed to determine which solution is stable by depending on the sign of the eigenvalues. Based on this analysis, the results indicate that the upper branch solution (first solution) is linearly stable, while the lower branch solution (second solution) is linearly unstable.

**Keywords:** Dual solutions, nanofluid, rotating flow, shrinking sheet, stability analysis.

**ABSTRAK** Aliran putaran lapisan sempadan terhadap permukaan mengecut yang telap di dalam nanobendalir dikaji. Penjelmaan keserupaan digunakan untuk menjelmakan persamaan perbezaan separa kepada persamaan perbezaan biasa tak linear. Kemudian, persamaan ini diselesaikan dengan menggunakan pakej bvp4c dalam perisian MATLAB. Keputusan menunjukkan bahawa terdapat lebih daripada satu penyelesaian yang disebut penyelesaian dwi diperolehi untuk julat tertentu bagi parameter putaran dan sedutan. Analisis kestabilan dijalankan untuk menentukan penyelesaian mana yang stabil dengan bergantung kepada tanda nilai eigen. Berdasarkan analisis ini, keputusan menunjukkan bahawa penyelesaian cabang atas (penyelesaian pertama) adalah stabil, sementara penyelesaian cabang bawah (penyelesaian kedua) adalah tidak stabil.

---

### INTRODUCTION

Along with the development of technology in this day and age, the usage of nanofluid became one of the hot issues to some

researchers in fluid mechanics. This issue attracts researchers because conventional heat transfer fluids like ethylene glycol, oil and water have poor thermal performance in a cooling system. By using such fluid as a

cooling tool will definitely enhance the manufacturing processes as well as operating costs. This fluid is formed by dispersing some of the nanoparticles into the base fluid which is water. After the discovery of nanofluid by Choi (1995), Bachok et al. (2010, 2012), Reddy et al. (2013), Das et al. (2014), Rosca and Pop (2014), Naramgari and Sulochana (2016) and Othman et al. (2017) have attempted to focus their research on the boundary layer flow of nanofluid using different effects and surfaces. Recently, the nanofluid problem with the presence of rotation in the flow is investigated by Nadeem et al. (2014) using two types of nanoparticles, namely, copper and titania over a stretching surface.

However, up to today, there are still only a few studies regarding a stability analysis of the dual solutions for the boundary layer flow and heat transfer. The idea and procedure to determine the stability of the solutions obtained has been triggered by Merkin (1985). This analysis later was continued by Weidman et al. (2006), Harris et al. (2009), Mahapatra and Nandy (2011), Sharma et al. (2014), Hafidzuddin et al. (2015), Najib et al. (2016) and Yasin et al. (2017). They concluded that the upper branch solution is always stable and

physically realizable, while the lower branch solution is not.

The main focus of the present paper is to continue the work of Nadeem et al. (2014) by considering the influence of suction using a different surface, which is the shrinking surface. The effect of the involved parameter is numerically analyzed and has been elaborated in particular for the characteristics of fluid flow and heat transfer. The `bvp4c` package is implemented in MATLAB software in order to compute the numerical results as well as to confirm the upper branch solution is stable, while the lower branch solution is not.

### FORMULATION OF THE PROBLEM

In this study, a steady three-dimensional rotating boundary layer flow in nanofluid past a shrinking sheet at  $z=0$  is considered by taking into account the effect of suction at the surface. The velocity components corresponding to  $x$ ,  $y$  and  $z$  directions are given by  $u$ ,  $v$  and  $w$ , respectively.  $\bar{\Omega}$  is denoted as the angular velocity of the rotating fluid in  $z$  direction and  $T$  is the temperature of the fluid. Based on the following assumptions, the governing equations for the mass, momentum and energy can be written as:

$$\frac{\partial u}{\partial x} + \frac{\partial v}{\partial y} + \frac{\partial w}{\partial z} = 0, \tag{1}$$

$$u \frac{\partial u}{\partial x} + v \frac{\partial u}{\partial y} + w \frac{\partial u}{\partial z} - 2\bar{\Omega}v = \frac{\mu_{nf}}{\rho_{nf}} \frac{\partial^2 u}{\partial z^2}, \tag{2}$$

$$u \frac{\partial v}{\partial x} + v \frac{\partial v}{\partial y} + w \frac{\partial v}{\partial z} + 2\bar{\Omega}u = \frac{\mu_{nf}}{\rho_{nf}} \frac{\partial^2 v}{\partial z^2}, \tag{3}$$

$$u \frac{\partial T}{\partial x} + v \frac{\partial T}{\partial y} + w \frac{\partial T}{\partial z} = \alpha_{nf} \frac{\partial^2 T}{\partial z^2}, \tag{4}$$

The boundary conditions for the Equations (1)-(4) are

$$\begin{aligned} u = U(x), v = 0, w = -w_0, T = T_w \text{ at } z = 0, \\ u \rightarrow 0, v \rightarrow 0, T \rightarrow T_\infty \text{ as } z \rightarrow \infty. \end{aligned} \tag{5}$$

We assume the surface is being shrunk with the velocity  $U(x) = ax$  in which  $a < 0$  is a constant,  $w_0$  is the constant mass flux with  $w_0 > 0$  for injection, while  $w_0 < 0$  for suction. Besides,  $T_\infty$  is the temperature outside the boundary layer and  $T_w$  is the temperature at the wall.  $\mu_{nf}$ ,  $\alpha_{nf}$ ,  $\rho_{nf}$  and

$k_{nf}$  are dynamic viscosity, thermal diffusivity, density and thermal conductivity of nanofluid and  $k_f$  is the thermal conductivity of the base fluid. The above mentioned parameters relate to the nanoparticle volume fraction,  $\phi$  are as follows:

$$\begin{aligned} \mu_{nf} = \frac{\mu_f}{(1-\phi)^{2.5}}, \alpha_{nf} = \frac{k_{nf}}{(\rho C_p)_{nf}}, \frac{k_{nf}}{k_f} = \frac{(k_s + 2k_f) - 2\phi(k_f - k_s)}{(k_s + 2k_f) + \phi(k_f - k_s)}, \\ \rho_{nf} = (1-\phi)\rho_f + \phi\rho_s, (\rho C_p)_{nf} = (1-\phi)(\rho C_p)_f + \phi(\rho C_p)_s, \end{aligned} \tag{6}$$

where  $\rho C_p$  refers to volumetric heat capacity,  $\rho_f$  and  $\mu_f$  are the density and dynamic viscosity of the base fluid, respectively, and  $k_s$  is the thermal conductivity of solid nanoparticles.

Equation (1) is satisfied and Equations (2)-(4) with the conditions (5) can be written in a simpler form by using the linear similarity transformations below:

$$u = axf'(\eta), v = axh(\eta), w = -\sqrt{av_f f(\eta)}, \eta = z\sqrt{\frac{a}{v_f}}, \theta(\eta) = \frac{T - T_\infty}{T_w - T_\infty}. \tag{7}$$

Next, Equations (6) and (7) are substituted into Equations (2)-(4) to obtain the following ordinary differential equations below:

$$\frac{1}{(1-\phi)^{2.5} [(1-\phi) + \phi(\rho_s / \rho_f)]} f''' + ff'' - f'^2 + 2\Omega h = 0, \tag{8}$$

$$\frac{1}{(1-\phi)^{2.5} [(1-\phi) + \phi(\rho_s / \rho_f)]} h'' + fh' - hf' - 2\Omega f' = 0, \tag{9}$$

$$\frac{k_{nf}/k_f}{Pr [(1-\phi) + \phi(\rho C_p)_s / (\rho C_p)_f]} \theta'' + f\theta' = 0, \tag{10}$$

and the conditions (5) become

$$\begin{aligned} f(0) = S, f'(0) = -1, h(0) = 0, \theta(0) = 1, \\ f'(\eta) \rightarrow 0, h(\eta) \rightarrow 0, \theta(\eta) \rightarrow 0 \text{ as } \eta \rightarrow \infty. \end{aligned} \quad (11)$$

In the above equations, primes refer to differentiation with respect to similarity variable,  $\eta$  and the Prandtl number is defined as  $Pr = \nu_f / \alpha_f$ . Besides that, the rotation and constant mass flux parameters are given by  $\Omega = \bar{\Omega} / a$  and  $S$ , respectively,

where  $S < 0$  for injection and  $S > 0$  for suction.

The skin friction coefficients in terms of wall shear stresses and the heat transfer coefficient in terms of Nusselt number can be expressed as:

$$Cf_x = \mu_{nf} (\partial u / \partial z)_{z=0} / \rho(ax)^2 = \frac{1}{(1-\phi)^{2.5}} Re_x^{-1/2} f''(0), \quad (12)$$

$$Cf_y = \mu_{nf} (\partial v / \partial z)_{z=0} / \rho(ax)^2 = \frac{1}{(1-\phi)^{2.5}} Re_x^{-1/2} h'(0), \quad (13)$$

$$Nu_x = -xk_{nf} (\partial T / \partial z)_{z=0} / k_f (T_w - T_\infty) = \frac{-k_{nf}}{k_f} Re_x^{1/2} \theta'(0), \quad (14)$$

where  $Re_x = Ux / \nu_f$  is the local Reynold number and  $Nu_x$  is the local Nusselt number.

### FORMULATION FOR STABILITY ANALYSIS

The first step to perform a stability analysis is to consider the problem in unsteady case. Hence, Equations (2)-(4) are substituted by

$$\frac{\partial u}{\partial t} + u \frac{\partial u}{\partial x} + v \frac{\partial u}{\partial y} + w \frac{\partial u}{\partial z} - 2\bar{\Omega}v = \frac{\mu_{nf}}{\rho_{nf}} \frac{\partial^2 u}{\partial z^2}, \quad (15)$$

$$\frac{\partial v}{\partial t} + u \frac{\partial v}{\partial x} + v \frac{\partial v}{\partial y} + w \frac{\partial v}{\partial z} + 2\bar{\Omega}u = \frac{\mu_{nf}}{\rho_{nf}} \frac{\partial^2 v}{\partial z^2}, \quad (16)$$

$$\frac{\partial T}{\partial t} + u \frac{\partial T}{\partial x} + v \frac{\partial T}{\partial y} + w \frac{\partial T}{\partial z} = \alpha_{nf} \frac{\partial^2 T}{\partial z^2}, \quad (17)$$

where  $t$  refers the time. From Equation (7), the new dimensionless variables for unsteady problem take place as:

$$u = axf'(\eta, \tau), v = axh(\eta, \tau), w = -\sqrt{av_f f(\eta, \tau)}, \eta = z \sqrt{\frac{a}{\nu_f}}, \theta(\eta, \tau) = \frac{T - T_\infty}{T_w - T_\infty}, \tau = \frac{Ut}{x}. \quad (18)$$

Substituting Equation (18) into Equations (15)-(17), we obtain the following:

$$\frac{1}{(1-\phi)^{2.5} [(1-\phi) + \phi(\rho_s / \rho_f)]} \frac{\partial^3 f}{\partial \eta^3} + f \frac{\partial^2 f}{\partial \eta^2} - \left( \frac{\partial f}{\partial \eta} \right)^2 - \frac{\partial^2 f}{\partial \eta \partial \tau} + 2\Omega h = 0, \quad (19)$$

$$\frac{1}{(1-\phi)^{2.5} [(1-\phi) + \phi(\rho_s / \rho_f)]} \frac{\partial^2 h}{\partial \eta^2} + f \frac{\partial h}{\partial \eta} - h \frac{\partial f}{\partial \eta} - \frac{\partial h}{\partial \tau} - 2\Omega \frac{\partial f}{\partial \eta} = 0, \quad (20)$$

$$\frac{k_{nf} / k_f}{\text{Pr} [(1-\phi) + \phi(\rho C_p)_s / (\rho C_p)_f]} \frac{\partial^2 \theta}{\partial \eta^2} + f \frac{\partial \theta}{\partial \eta} - \frac{\partial \theta}{\partial \tau} = 0, \quad (21)$$

subject to the boundary conditions

$$f(0, \tau) = S, \quad \frac{\partial f}{\partial \eta}(0, \tau) = -1, \quad h(0, \tau) = 0, \quad \theta(0, \tau) = 1, \quad (22)$$

$$\frac{\partial f}{\partial \eta}(\eta, \tau) \rightarrow 0, \quad h(\eta, \tau) \rightarrow 0, \quad \theta(\eta, \tau) \rightarrow 0 \quad \text{as } \eta \rightarrow \infty.$$

Furthermore, to identify the stability of the steady flow solution  $f(\eta) = f_0(\eta)$ ,  $h(\eta) = h_0(\eta)$  and  $\theta(\eta) = \theta_0(\eta)$  which complying the boundary value problem (19)-(22), we assume

$$f(\eta, \tau) = f_0(\eta) + e^{-\gamma\tau} F(\eta, \tau), \quad h(\eta, \tau) = h_0(\eta) + e^{-\gamma\tau} H(\eta, \tau), \quad (23)$$

$$\theta(\eta, \tau) = \theta_0(\eta) + e^{-\gamma\tau} G(\eta, \tau),$$

where  $\gamma$  is an unknown eigenvalue,  $F(\eta, \tau)$ ,  $H(\eta, \tau)$  and  $G(\eta, \tau)$  are small relative to  $f_0(\eta)$ ,  $h_0(\eta)$  and  $\theta_0(\eta)$ , respectively. Substituting Equation (23) into Equations (19)-(22), we obtain the linearized problem

$$\frac{1}{(1-\phi)^{2.5} [(1-\phi) + \phi(\rho_s / \rho_f)]} \frac{\partial^3 F}{\partial \eta^3} + f_0 \frac{\partial^2 F}{\partial \eta^2} + F \frac{\partial^2 f_0}{\partial \eta^2} - 2 \frac{\partial f_0}{\partial \eta} \frac{\partial F}{\partial \eta} + \gamma \frac{\partial F}{\partial \eta} - \frac{\partial^2 F}{\partial \eta \partial \tau} + 2\Omega h = 0, \quad (24)$$

$$\frac{1}{(1-\phi)^{2.5} [(1-\phi) + \phi(\rho_s / \rho_f)]} \frac{\partial^2 H}{\partial \eta^2} + f_0 \frac{\partial H}{\partial \eta} + F \frac{\partial h_0}{\partial \eta} - H \frac{\partial f_0}{\partial \eta} - h_0 \frac{\partial F}{\partial \eta} + \gamma H - \frac{\partial H}{\partial \tau} - 2\Omega \frac{\partial F}{\partial \eta} = 0, \quad (25)$$

$$\frac{k_{nf} / k_f}{\text{Pr} [(1-\phi) + \phi(\rho C_p)_s / (\rho C_p)_f]} \frac{\partial^2 G}{\partial \eta^2} + f_0 \frac{\partial G}{\partial \eta} + F \frac{\partial \theta_0}{\partial \eta} + \gamma G - \frac{\partial G}{\partial \tau} = 0, \quad (26)$$

together with the boundary conditions

$$F(0, \tau) = 0, \frac{\partial F}{\partial \eta}(0, \tau) = 0, H(0, \tau) = 0, G(0, \tau) = 0, \tag{27}$$

$$\frac{\partial F}{\partial \eta}(\eta, \tau) \rightarrow 0, H(\eta, \tau) \rightarrow 0, G(\eta, \tau) \rightarrow 0 \text{ as } \eta \rightarrow \infty.$$

As discussed by Weidman et al. (2006), we are setting  $\tau = 0$  to identify the initial growth or decay of the solution (23). Thus, functions  $F = F_0(\eta)$ ,  $H = H_0(\eta)$  and  $G = G_0(\eta)$ . To test our numerical method, we consider the following linear eigenvalue problems

$$\frac{1}{(1-\phi)^{2.5} [(1-\phi) + \phi(\rho_s / \rho_f)]} F_0''' + f_0 F_0'' + f_0'' F_0 - 2f_0' F_0' + \gamma F_0'' + 2\Omega H_0 = 0, \tag{28}$$

$$\frac{1}{(1-\phi)^{2.5} [(1-\phi) + \phi(\rho_s / \rho_f)]} H_0'' + f_0 H_0' + F_0 h_0' - f_0' H_0 - F_0' h_0 + \gamma H_0 - 2\Omega F_0' = 0, \tag{29}$$

$$\frac{k_{mf} / k_f}{Pr [(1-\phi) + \phi(\rho C_p)_s / (\rho C_p)_f]} G_0'' + f_0 G_0' + F_0 \theta_0' + \gamma G_0 = 0, \tag{30}$$

together with the new conditions

$$F_0(0) = 0, F_0'(0) = 0, H_0(0) = 0, G_0(0) = 0, \tag{31}$$

$$F_0'(\eta) \rightarrow 0, H_0(\eta) \rightarrow 0, G_0(\eta) \rightarrow 0 \text{ as } \eta \rightarrow \infty.$$

We should note that for a certain value of  $Pr$  and  $\gamma$ , the stability of the steady flow solutions  $f_0(\eta)$ ,  $h_0(\eta)$  and  $\theta_0(\eta)$  is identified by the smallest eigenvalues. These smallest eigenvalues give two solutions, first is a negative solution and second is a positive solution. For the negative eigenvalue, there is an initial growth of interruption and the flow is said to be unstable. Meanwhile, for the positive eigenvalue, there is an initial decomposition and the flow is said to be stable. Based on the previous study by Harris et al. (2009), they suggest that the range of the possible eigenvalues can be computed by relaxing a boundary condition on  $F_0(\eta)$ ,  $H_0(\eta)$  or  $G_0(\eta)$ . In the present study, we solve the eigenvalue problems (28)-(31) by selecting

the condition  $F_0'(\eta) \rightarrow 0$  as  $\eta \rightarrow \infty$  which later changes to the new condition  $F_0''(0) = 1$ .

## RESULT AND DISCUSSIONS

In order to give an understanding of the current problem, the numerical computations are carried out for the selected parameters of interest, including, rotation  $\Omega$ , nanoparticle volume fraction  $\phi$  and suction  $S$  parameters. The Equations (8)-(10) with conditions (11) are solved using `bvp4c` function in MATLAB software. The range of values of  $\phi$  is between 0 to 0.2, where  $\phi = 0$  corresponding to a regular fluid and

$Pr = 6.2$  (water). The thermophysical properties of the copper (Cu), titania ( $TiO_2$ ), alumina ( $Al_2O_3$ ) and the base fluid are given in the work of Oztop and Abu-Nada (2008). Figures 1 (a) to (c) present the effect of nanoparticle volume fraction  $\phi$  on the variation of the skin friction coefficient of  $x$  and  $y$  components,  $f''(0)$  and  $h'(0)$  and the local Nusselt number  $-\theta'(0)$  with suction parameter for Cu-water nanofluid when  $\Omega = 0.001$ . It is found that the magnitude of the skin friction coefficients for both components increase

with an increment in the value of  $\phi$ . The fact that the presence of nanoparticles in the base fluid will accelerate the fluid motion due to the collision between the nanoparticles and base fluid particle. Thus, decreasing the momentum boundary layer thickness and consequently, increasing the skin frictions at the surface. Furthermore, the opposite trend is observed for the local Nusselt number as the  $\phi$  increase. It should be noted that the critical values of suction seem to decrease as the  $\phi$  increase.

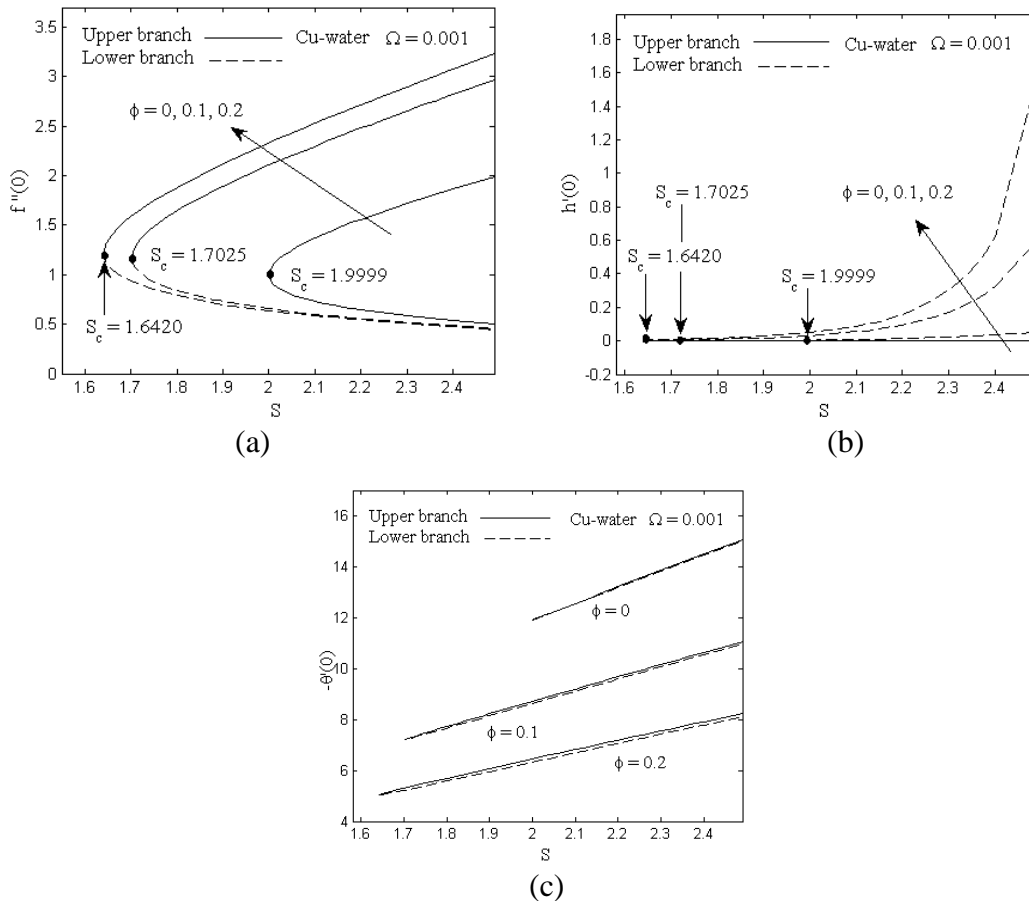


**Figure 1.** (a-c) Effect of nanoparticle volume fraction  $\phi$  on the skin friction coefficient of  $x$  and  $y$  components and local Nusselt number.

Figures 2 (a) to (c) illustrate the influence of the rotation  $\Omega$  on the variation of the  $f''(0)$ ,  $h'(0)$  and  $-\theta'(0)$  with suction parameter for  $\text{TiO}_2$  when  $\phi = 0.2$ . From these figures, the magnitude of the  $f''(0)$ ,  $h'(0)$  and  $-\theta'(0)$  are noticed to increase when the values of the rotation increase. However, the dual solutions exist when  $\Omega = 0.001$  for  $S_c > 2.0564$ , while beyond this limit no

solutions exist.  $S_c$  is the critical value of suction for which Equations (8)-(10) have no solutions. It is worth mentioning that increasing the rotation in the flow reduces the momentum boundary layer thickness. Consequently, increases both the skin friction coefficients of  $x$  and  $y$  components on the wall.

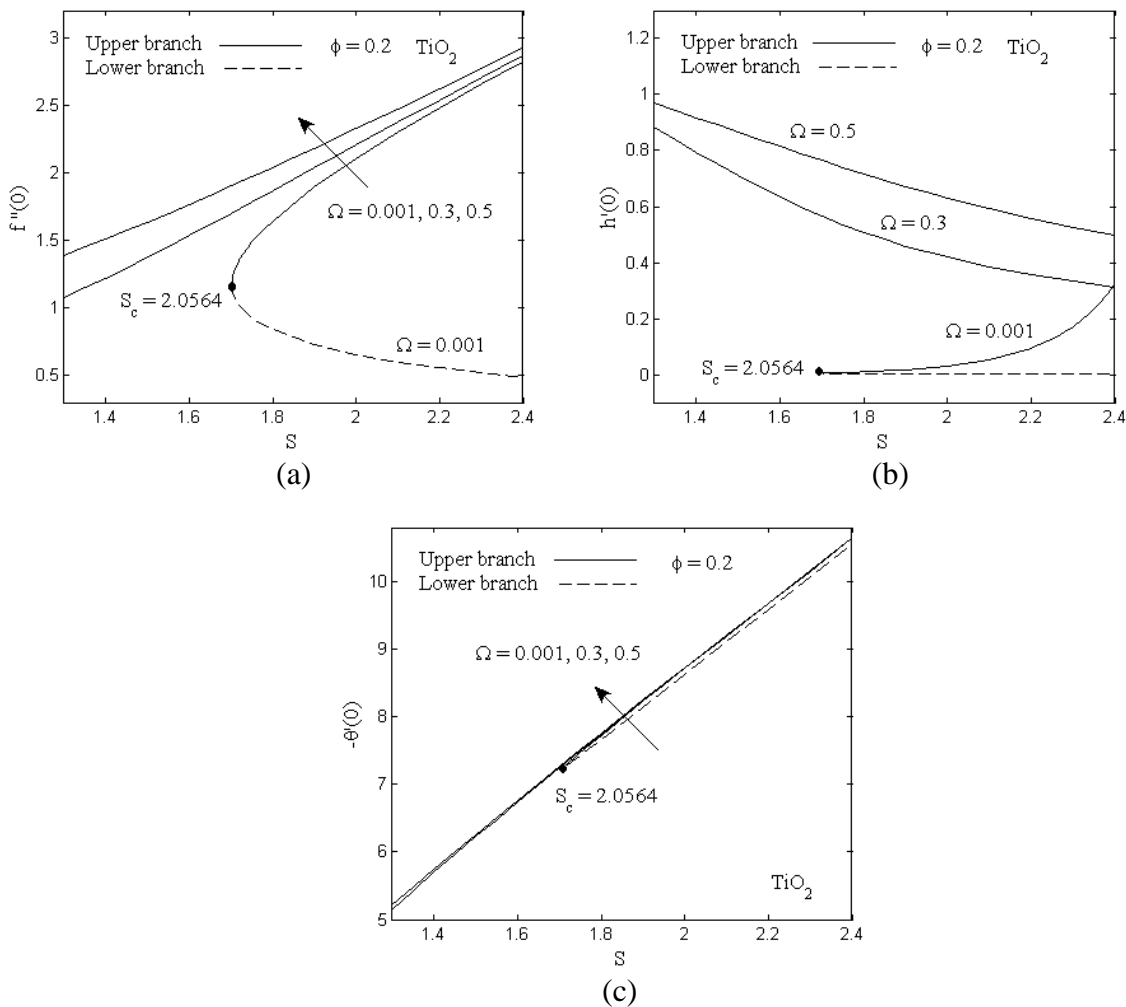


**Figure 2.** (a-c) Effect of rotation  $\Omega$  on skin friction coefficients of  $x$  and  $y$  components and local Nusselt number.



Figures 3 and 4 demonstrate the effects of the velocities of  $x$  and  $y$  components,  $f'(\eta)$ ,  $h(\eta)$  and the temperature profiles  $\theta(\eta)$ . All the profiles are plotted to validate the numerical results obtained in the current study. It is shown that all profiles have satisfied the boundary conditions (11)

the different nanoparticles and suction parameter on asymptotically with different patterns of graphs. As we noticed, the thickness of the boundary layer for the lower branch solution is always thicker than the upper branch solution.

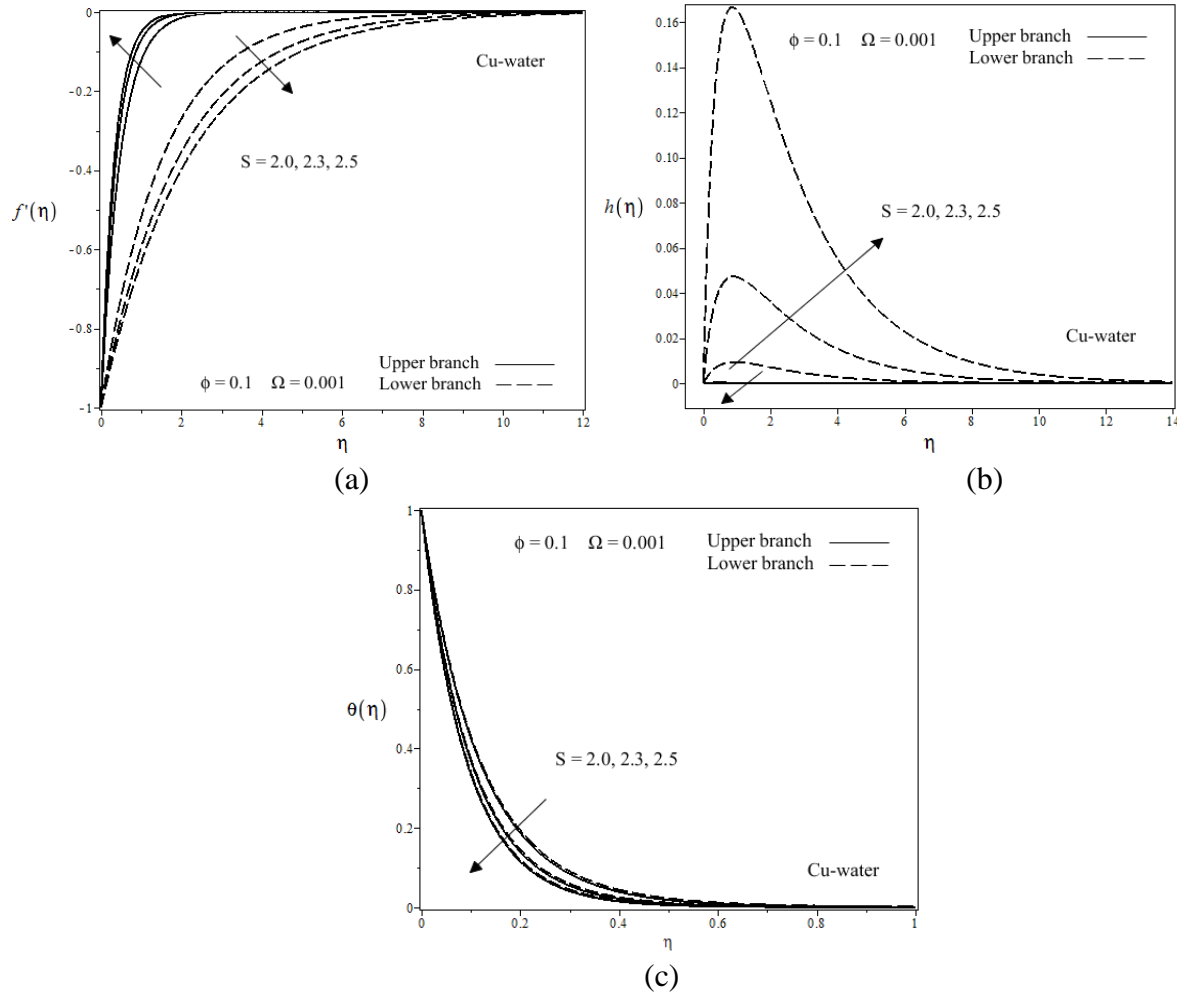


**Figure 3.** (a-c) Effect of suction  $S$  on the velocity of  $x$  and  $y$  components and temperature profiles.

From this study, the stability of the dual solutions are identified using `bvp4c` function in MATLAB software. This analysis is conducted to know which of the upper or lower branch solution is linearly stable by depending on the sign of the smallest eigenvalues obtained. The unknown eigenvalue is introduced in Equation (23) and to determine the values of  $\gamma$ , the linear eigenvalue problems given in Equations (28)-(30) subjected to the conditions (31) is being applied. Table 1 and 2 displays the smallest eigenvalues  $\gamma$  for different values

of the selected parameters of interest. From the tables, the positive value of  $\gamma$  represents an initial decay of disturbance and the flow is said to be stable for the upper branch solution. Meanwhile, the negative value of  $\gamma$  refers to an initial growth of disturbance and the flow is an unstable for the lower branch solution. The stable flow is always given a good physical meaning that can be realized.

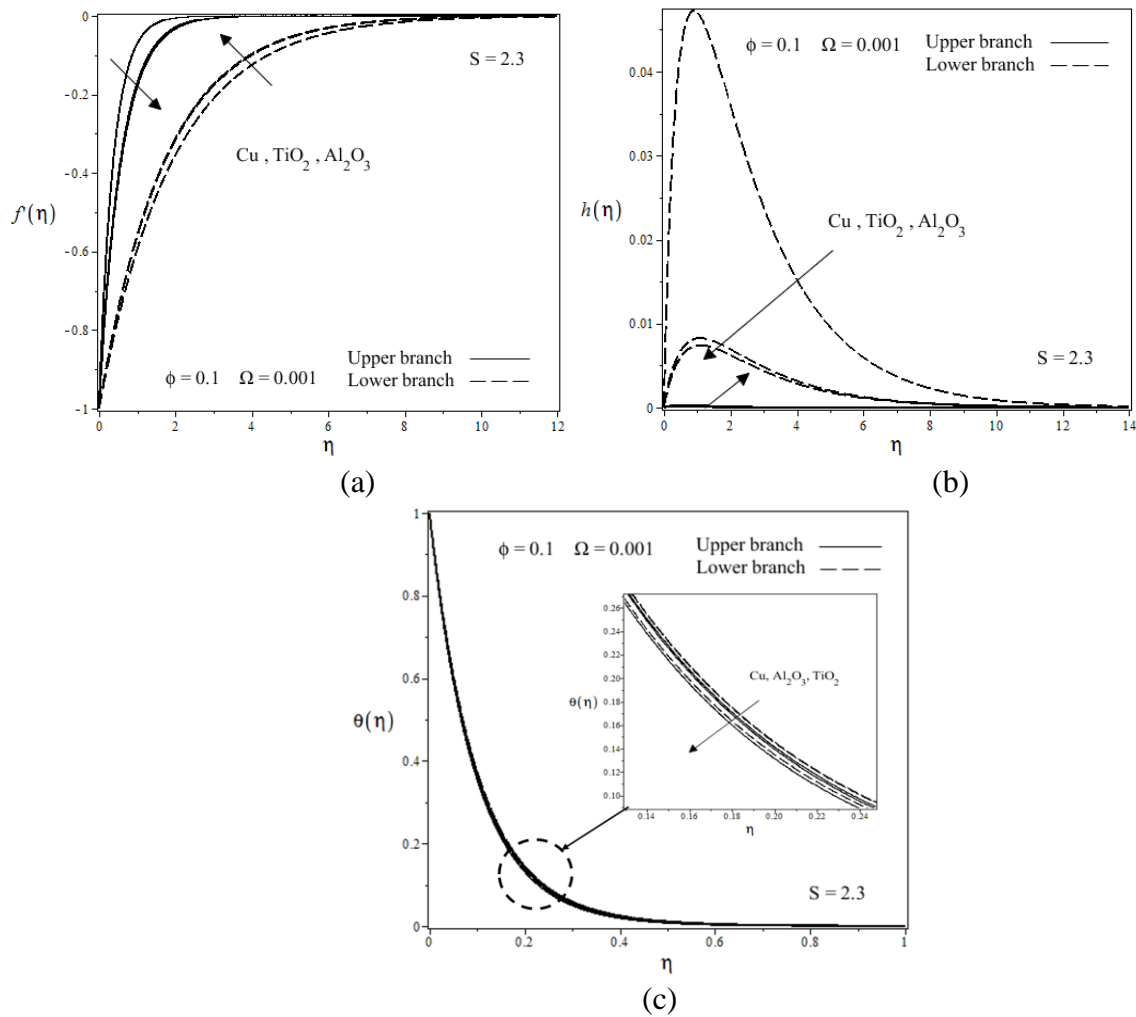


**Figure 4.** (a-c) Effect of nanoparticles on the velocity of  $x$  and  $y$  components and temperature profiles.

**Table 1.** Smallest eigenvalues  $\gamma$  for various values of  $\Omega$  and  $S$  when  $\phi = 0.1$  for Cu-water nanofluid.

$\Omega$	$S$	Upper branch	Lower branch
0.0	2.1	0.9921	-0.6365
	2.2	1.1591	-0.6890
	2.3	1.3277	-0.7328
0.001	2.1	0.9922	-0.0352
	2.2	1.1593	-0.0211
	2.3	1.3279	-0.0104
0.1	2.1	1.3905	-
	2.2	1.5495	-
	2.3	1.7131	-

**Table 2.** Smallest eigenvalues  $\gamma$  for various values of  $\phi$  and  $S$  using a different nanoparticles when  $\Omega = 0.001$ .

Nanoparticles	$\phi$	$S$	Upper branch	Lower branch
Copper	0	2.1	0.4041	-0.3356
		2.2	0.5957	-0.4549
		2.3	0.7574	-0.5378
	0.1	2.1	0.9922	-0.0352
		2.2	1.1593	-0.0211
		2.3	1.3279	-0.0104
	0.2	2.1	1.1186	-0.0247
		2.2	1.2878	-0.0131
		2.3	1.4707	-0.0045
Alumina	0	2.1	0.4041	-0.3356
		2.2	0.5957	-0.4549
		2.3	0.7574	-0.5378
	0.1	2.1	0.3984	-0.3316
		2.2	0.5911	-0.4522
		2.3	0.7531	-0.5358
	0.2	2.1	0.1042	-0.0972
		2.2	0.4119	-0.3400
		2.3	0.5954	-0.4534
Titania	0	2.1	0.4041	-0.3356
		2.2	0.5957	-0.4549
		2.3	0.7574	-0.5378
	0.1	2.1	0.4463	-0.3642
		2.2	0.6306	-0.4744
		2.3	0.7903	-0.5531
	0.2	2.1	0.2557	-0.2258
		2.2	0.4869	-0.3894
		2.3	0.6590	-0.4884

## CONCLUSION

In this paper, the effect of the nanoparticles volume fraction, rotation and suction parameters on the fluid flow and heat transfer analysis of the rotating flow past a shrinking surface in nanofluid is investigated. The stability analysis is performed to identify the stability of the solutions obtained. Some discussions that can be made are as follows:

- Dual solutions exist when the values of rotation are small enough, says  $\Omega = 0.001$  for  $S_c > 2.0564$  and beyond this limit no solutions exist for  $\text{TiO}_2$ .
- The highest values of heat transfer occur for Cu compared to  $\text{Al}_2\text{O}_3$  and  $\text{TiO}_2$  due to it has higher thermal conductivity than others.
- The upper branch solution is stable and physically realizable compared to the lower branch solution.
- Increasing the rotation parameter gives rise the magnitudes of the skin friction coefficients and the local Nusselt number.
- Increasing the nanoparticles volume fraction parameter leads to an increase in the skin friction coefficients, while the opposite trend is found for the local Nusselt number.

## ACKNOWLEDGEMENT

The authors gratefully acknowledged the financial support received from Ministry of Higher Education Malaysia in the form of Fundamental Research Grant Scheme (FRGS/1/2018/STG06/UPM/02/4/5540155) and Putra Grant GP-IPS/2018/9667900 from Universiti Putra Malaysia.

## REFERENCES

- Bachok, N., Ishak, A., & Pop, I. (2010). Boundary-layer flow of nanofluids over a moving surface in a flowing fluid. *International Journal of Thermal Sciences*, 49:1663-1668.
- Bachok, N., Ishak, A., & Pop, I. (2012). Unsteady boundary-layer flow and heat transfer of a nanofluid over a permeable stretching/shrinking sheet. *International Journal of Heat and Mass Transfer*, 55:2102-2109.
- Choi, S. U. S. (1995). Enhancing thermal conductivity of fluids with nanoparticles. *ASME Publication*, 231:99-105.
- Das, K., Duari, P. R., Pop, I., & Kundu, P. K. (2014). Nanofluid flow over an unsteady stretching surface in presence of thermal radiation. *Alexandria Engineering Journal*, 53:737-745.

- Hafidzuddin, E. H., Nazar, R., Arifin, N. M., & Pop, I. (2015). Stability analysis of unsteady three-dimensional viscous flow over a permeable stretching/shrinking surface. *Journal of Quality Measurement and Analysis*, 11:19-31.
- Harris, S. D., Ingham, D. B., & Pop, I. (2009). Mixed convection boundary-layer flow near the stagnation point on a vertical surface in a porous medium: Brinkman model with slip. *Transport Porous Media*, 77: 267-285.
- Mahapatra, T. R. & Nandy, S. K. (2011). Stability analysis of dual solutions in stagnation-point flow and heat transfer over a power-law shrinking surface. *International Journal of Nonlinear Sciences*, 12: 86-94.
- Merkin, J. H. (1985). On dual solutions occurring in mixed convection in a porous medium. *Journal of Engineering Mathematics*, 20:171-179.
- Nadeem, S., Rehman, A., & Mehmood, R. (2014). Boundary layer flow of rotating two phase nanofluid over a stretching surface. *Heat Transfer Asian Research*, 45:285-2
- Najib, N., Bachok, N., & Ari\_n, N. M. (2016). Stability of dual solutions in boundary layer flow and heat transfer over an exponentially shrinking cylinder. *Indian Journal of Science and Technology*, 9:1-6.
- Naramgari, S. & S ulochana, C. (2016). MHD flow over a permeable stretching/shrinking sheet of a nanofluid with suction/injection. *Alexandria Engineering Journal*, 55:819-827
- Othman, N. A., Yacob, N. A., Bachok, N., Ishak, A., & Pop, I. (2017). Mixed convection boundary-layer stagnation point flow past a vertical stretching/shrinking surface in a nanofluid. *Applied Thermal Engineering*, 115:1412-1417.
- Oztop, H. F. & Abu-Nada, E. (2008). Numerical study of natural convection in partially heated rectangular enclosures filled with nanofluids. *International Journal of Heat Fluid Flow*, 29:1326-1336.
- Reddy, C. R., Murthy, P. V. S. N., Chamkha, A. J., & Rashad, A. M. (2013). Soret effect on mixed convection flow in a nanofluid under convective boundary condition. *International Journal of Heat and Mass Transfer*, 64:384-392.
- Rosca, N. C. & Pop, I. (2014). Unsteady boundary layer flow of a nanofluid past a moving surface in an external uniform free stream using Buongiorno's model. *Computers and Fluids*, 95:49-55.
- Sharma, R., Ishak, A., & Pop, I. (2014). Stability analysis of magnetohydrodynamic stagnation-point flow toward a stretching/shrinking sheet. *Computers and Fluids*, 102:94-98.

Weidman, P. D., Kubitschek, D. G., & Davis, A. M. J. (2006). The effect of transpiration on self-similar boundary layer flow over moving surfaces. *International Journal of Engineering Sciences*, 44:730-737.

Yasin, M. H. M., Ishak, A., & Pop, I. (2017). Boundary layer flow and heat transfer past a permeable shrinking surface embedded in a porous medium with a second-order slip: A stability analysis. *Applied Thermal Engineering*, 115:1407-1]